Published in final edited form as:
J Comp Neurol. 2003 September 15; 464(2): 115–130. doi:10.1002/cne.10772.

Vocal Circuitry in *Xenopus laevis*: Telencephalon to Laryngeal Motor Neurons

CATHERINE J. BRAHIC and **DARCY B. KELLEY***
Department of Biological Sciences, Columbia University, New York, New York 10027

Abstract

Sexually differentiated calling patterns of *Xenopus laevis* are conveyed to the vocal organ by a dedicated neuromuscular system. Here, we define afferents to vocal motor neurons and determine whether the connectivity of the vocal pathway is sexually differentiated. The use of fluorescent dextran amines and the isolated brain preparation readily permitted identification of anterograde and retrograde connectivity patterns. The whole-mount preparation allowed us to observe projections in their entirety, including cells of origin of a projection (for retrograde projections), terminal fields (for anterograde connections), and fiber tracts. Major findings are the confirmation of a robust and reciprocal connection between cranial nucleus (n.) IX-X and the pretrigeminal nucleus of the dorsal tegmental area of the medulla (DTAM) as well as between DTAM and the ventral striatum (VS). Newly revealed is the extensive connectivity between the rostral subdivision of the dorsal nucleus raphe (rRpd) and candidate vocal nuclei. In contrast to previous results using peroxidase, we did not observe dramatic sex differences in connectivity, although some connections were less robust in female than in male brains. Some retrograde connections previously observed (e.g., anterior preoptic area to DTAM) were not confirmed. Plausible hypotheses are that a set of rhombencephalic neurons located in DTAM, the inferior reticular formation and n.IX-X are responsible for generating patterned vocal activity, that activity is modulated by neurons in rRpd, and that activity in VS (particularly that evoked by conspecific calls), together with effects of steroid hormones at many sites in the vocal circuit, contribute to the initiation of calling.

Indexing terms

nucleus ambiguus; frog; song; raphe; parabrachial nucleus

Male and female South African clawed frogs, *Xenopus laevis*, use a rich repertoire of vocalizations in intraspecies communication (Kelley and Tobias, 1999). Calls are made up of click trains (trills) and different call types are distinguished by trill rate, temporal structure, and intensity modulation. We wish to understand how these calls are generated by the central nervous system and how sexually differentiated properties are produced. In this study, we use neuroanatomic tracing methods to define afferents to vocal motor neurons in both sexes and to determine whether the connectivity of the vocal pathway is sexually differentiated.

Clicks are produced by contractions of intrinsic laryngeal muscles in response to the activity of the laryngeal nerves (Tobias and Kelley, 1987). Recordings from these nerves in

*Correspondence to: Darcy B. Kelley, MC2432, Department of Biological Sciences, 911 Fairchild, Columbia University, New York, NY 10027. dbk3@columbia.edu.

vocalizing male and female frogs reveal sexually distinct patterns that correspond closely to those of actual vocalizations (Yamaguchi and Kelley, 2000). Sex-specific vocal patterns are thus produced within the central nervous system. The laryngeal motor neurons are located in cranial nerve nucleus IX-X (n.IX-X) of the caudal medulla (Kelley, 1980) that contains both motoneurons and inter-neurons (Simpson et al., 1986). Because vocal motorneurons do not, by themselves, generate sexually differentiated call rates and patterns (Yamaguchi et al., 2000), afferents to laryngeal motoneurons are likely candidates. Identification of these afferents is one goal of this study.

Sex differences in connectivity of vocal nuclei are common in several species of song bird and are believed to contribute to male-specific songs (Simpson and Vicario, 1990). This observation raises the possibility that sex differences in the vocal pathway may contribute to sex-typical vocalizations in frogs. In a previous study, we used iontophoretic application of the plant lectin, wheat germ agglutinin coupled to horseradish peroxidase (HRP-WGA), to examine afferents n.IX-X in both sexes (Wetzel et al., 1985). That study revealed that the laryngeal motor nucleus receives a major input from a nucleus in the rostral rhombencephalon, DTAM (the pretrigeminal nucleus of the dorsal tegmental area of the medulla). Injections of HRP-WGA into DTAM revealed that the connection was reciprocal but sexually dimorphic: the DTAM to n.IX-X projection appeared to be less robust in females as was an apparent projection from the preoptic area to DTAM.

There are several limitations to the observations of the study by Wetzel et al. First, HRP-WGA only labels retrogradely, yet retrograde labeling may depend on the functional strength of synapses (Holtzman et al., 1971; Jiang et al., 1993; Hosogai and Matsuo, 2002). In our system, this could be weaker in females than in males. Second, we could not rule out the possibility that some labeled cells arose from transneuronal transport, even at the short (2 days) survival time used (Gerfen et al., 1982). Finally, axon trajectories could not be described as the tissue was examined in sections, in accordance with conventional methodology. Axonal pathways frequently weave in and out of thin planes of section and are therefore rarely observed, especially in their entirety.

The development of fluorescent dextran amines for neuroanatomical tracing (Schmued et al., 1990) together with the adoption of an isolated brain preparation (Luksch et al., 1996) and whole-mount visualization of projections (this study), has enabled us to circumvent these limitations.

MATERIALS AND METHODS

The periventricular location of central nervous system (CNS) nuclei in *Xenopus laevis* and the complications of injections into brain regions covered by the choroid plexus led us to an in vitro approach using an isolated, perfused brain preparation (Luksch et al., 1996). Tracers were delivered either as small crystals or in solution by means of a picospritzer and placed by using external landmarks at locations and depths determined in a series of pilot experiments, which also determined optimal incubation times. We used Fluoro-Ruby (FR; tetramethylrhodamine dextran; anionic, lysine fixable, 3,000 molecular weight, Molecular Probes, D-3308) as the tracer because FR reliably labels both anterograde and retrograde projections in this in vitro preparation (Edwards and Kelley, 2001). After FR transport, isolated brains were fixed, dehydrated, cleared, and bisected in the sagittal plane. Injection sites, retrogradely labeled cells and terminal fields were documented in this whole-mount preparation, which was then paraffin embedded and sectioned to reveal cellular detail.

Thin, poorly myelinated axons can be very difficult to detect in sectioned material, especially in sparse projections or when background fluorescence (autofluorescence) is

present. An advantage of our approach is the ability to follow axonal trajectories in their entirety.

In vitro brain preparation

Adult male and female *Xenopus laevis* were purchased from Nasco (Fort Akinson, WI) and *Xenopus* One (Ann Arbor, MI). All animals were at stage PM6 (Tobias et al., 1991). Animal treatments followed the guidelines of the NIH and of Columbia's Institutional Animal Care and Use Committee. Deeply anesthetized frogs (ethyl-m-aminobenzoate, methane sulfonic acid, Sigma, 1.0 ml [males] or 2.0 ml [females] of a 1.3% solution injected into the dorsal lymph sac) were perfused transcardially with oxygenated saline (11 mM glucose, 75 mM NaCl, 25 mM $NaHCo_3$, 2 mM KCl, 0.5 mM $MgCl_2$, and 2 mM $CaCl_2$, pH7.3, Luksch et al. 1996; 20 ml in males, 30 ml in females) at 4°C. Immediately after perfusion, the spinal cord was severed, the skull removed and submerged in cold, freshly oxygenated saline. The brain was then exposed and pinned to a Sylgard-coated Petri dish filled with cold oxygenated saline. After tracer application, brains were maintained at 4°C for 3 days in continuously oxygenated saline; the saline was replaced every 24 hours. A previous study (Luksch et al., 1996) demonstrated good maintenance of electrophysiological parameters (i.e., resting membrane potentials) for up to 4 days in the oxygenated saline and no cellular degeneration. We confirmed the latter observation: as long as oxygen was supplied continuously, cellular integrity appeared intact.

Injections

Depending on the injection site, FR was delivered either as a crystal on the tip of a minuten pin or by pressure injection. In the former method (used for relatively super-ficial nuclei), a saturated FR solution in saline was prepared and a small drop allowed to dry on the tip of the pin (Fine Science Tools, no. 26002-10). The pin was mounted on the tip of a micropipette (Clay Adams, #4618) with 1/16 heat shrink tubing (3M, FP-301). "Spears" made in this manner were placed in a 1-cc syringe mounted on a micromanipulator (Narishige) for injections. In the latter method (used for deeper brain nuclei), FR (15% FR in saline) was back-loaded into borosilicate glass capillary tubing (1.0 mm OD × 0.75 mm ID/ fiber, FHC, Bowdoinham, ME, #30-30-0), pulled (Sutter Instrument Co., model P-87) to an external diameter of 20 μm and delivered by pressure (Picospritzer II, General Valve Corporation; 2– 6 pulses, 10 –20 psi, 15 msec). In both cases, the saline was lowered prior to injection and the surface of the brain dried with a small piece of Kimwipe.

In male and female brains, tracer injections were made into the anterior preoptic area (APOA; five males, five females), the pretrigeminal nucleus of the dorsal tegmental area of the medula (DTAM; three males, three females), the rostral raphe pars dorsalis (rRpd; four males, three females), and the motor nucleus of cranial nerve IX-X (n.IX-X; four males, five females). Neuroanatomical terminology used here is based on Kelley et al. (1975), Neary and Northcutt (1983), Nikundiwe and Nieuwenhuys (1983), and Wetzel et al. (1985).

The anterior preoptic area is immediately anterior to the posterior preoptic area (PPOA), which is in turn immediately anterior to the optic chiasm. The APOA wraps around the rostral extent of the preoptic recess and is caudal to the medial septum. If the meninges are carefully removed, the ventral extent of the preoptic recess is visible and FR can be applied at the rostral end of the recess, just below the brain surface (a ventral approach). To control for the possibility that transport from APOA might be a result of diffusion into neighboring septal nuclei, two control injections (one male and one female brain) were placed in APOA after the area between APOA and septum was transected.

Injections into APOA in both males and females gave rise to labeled cell bodies in the rostral extent of Raphe pars dorsalis (rRpd). To confirm the projection, we injected rRpd with FR.

Rostral Rpd is located on the midline, just anterior and ventral to the insertion of the trigeminal nerve. The cells labeled by injections into APOA were consistently located in the rostral 0.6 mm of the nucleus. Before each injection, the distance from the midline to the insertion of N.V, at the level of the junction of the tectum and the cerebellum, was measured (~1.2 mm). Brains were then pinned on their sides, and a FR-filled microelectrode was advanced at a point just rostral and ventral to the insertion of the trigeminal nerve until it reached the midline.

Nucleus DTAM is medial and caudal to nucleus isthmi (NI) and medial and rostral to the motor nucleus of V (n.V). Injections into DTAM were placed caudal to the junction of the cerebellum and the tectum, at the level of the anterodorsal corner of the fourth ventricle (~0.5 mm from the cerebellar midline), and 1.5 mm below the dorsal surface of the cerebellum.

The motor nucleus of IX-X extends caudally from the insertion site of the fourth root of nerve IX-X (N.IX-X), just caudal to the obex, to the rostral border of the spinal cord. In males, n.IX-X is located predominantly in the white matter, whereas in females, the nucleus is more medial. In both sexes, n.IX-X lies immediately lateral to the inferior reticular formation (Ri) and all n.IX-X injections included at least a portion of adjacent Ri. Because n.IX-X extends approximately 1 mm in the anterior-posterior plane, FR was applied as crystals from three minuten pins inserted just below the brain surface: one was placed immediately caudal to the insertion of the fourth root, the second rostral to the first and at the level of the obex, and the third equidistant between the first two.

Whole-mounts: fixation, dehydration, clearing, and sectioning

Brains were fixed overnight in 4% paraformaldehyde at 4°C. The dura and the pia matter were then removed, and the brain was transected mid-sagittally. The resulting half-brains were dehydrated in increasing concentrations of ethanol and cleared in methyl salicylate. Cleared half-brains are completely transparent. Cell bodies, fiber trajectories, and terminal fields can easily be observed under the fluorescence microscope. After injection sites and projections were documented, whole-mount brains were embedded in paraffin and cut on a rotary microtome at 25 μm. Sections were de-paraffinized in xylene, and cover-slipped with Cytoseal XYL (Stephens Scientific, Kalamazoo, MI), an anti-fading mounting medium.

Certain projections were confirmed in frozen-sectioned material. These brains were equilibrated in 20% sucrose, sectioned at 25 μm on a cryostat (Hacker Instrument Company), dehydrated, cleared, and examined.

Photomicrography

Photomicrographs were taken with a digital camera (Spot; Diagnostic Instruments, software version 3.02) and prepared for publication by using Adobe Photoshop. Whole-mount material was photographed through a coverslip while immersed in methyl salicylate in a depression well slide. Whole-mount material was then sectioned in the sagittal or transverse plane and labeled nuclei relocated in sections. The locations of labeled cells and terminal fields were confirmed in additional material sectioned in the horizontal plane (frozen sections) and mapped onto a series of horizontal reference sections that had been stained with cresyl violet to delimit boundaries of brain nuclei. Reference sections were photographed and scanned and photomontages prepared by using Adobe Photoshop. Brightness and contrast were adjusted to preserve the outline of the section and cellular

detail. Uneveness of illumination in the photomontages was adjusted by using the "smart blur" function (radius and threshold: 15.8).

RESULTS

Whole-mount preparation

The whole-mount preparation allowed us to observe projections in their entirety (Fig. 2A), including cells of origin of a projection (for retrograde projections; Fig. 1B), terminal fields (for anterograde connections; Fig. 1C), and fiber tracts (Fig. 1B–D, 2A). These were documented on photomicrographs, and the locations of label confirmed on sections of the same material. Specific labeled cells were readily recognizable both in whole-mounts and after subsequent sectioning (e.g., cell with asterisk in Fig. 1A). In the sagittal whole-mount preparation, fiber trajectories could easily be followed from the injection site, particularly for projections that traveled anteroposteriorly (Fig. 1B–D) or dorsoventrally (Fig. 2A). Because many axonal projections weave in and out of a single plane of section, trajectories are very difficult to trace in sections (cf. Fig. 2B).

Injections into n.IX-X

At the level of the injection site into n.IX-X and Ri (Fig. 3D), labeled cells and terminal fields were found in contralateral inferior reticular formation (Ri), as well as in ipsilateral ventral striatum (VS) and contralateral n.IX-X. In addition, the oculomotor nucleus (n.III) contained labeled cells contralaterally (illustrated in Fig. 1B). More dorsally (Fig. 3C), labeled cells and terminal fields extended into the medial reticular formation (Rm). The Raphe pars dorsalis (Rpd), including its rostral subdivision (rRpd), contained labeled terminal fields only (both ipsi-and contralaterally). Immediately dorsal (Fig. 3B), the nucleus tractus solitarius (nTS) contained labeled cells and terminal fields ipsilaterally as did the motor nucleus of V (n.V), contralaterally. A prominent projection to and from DTAM was present in dorsal medulla on both sides (Fig. 3A). Nucleus DTAM is most easily visualized in horizontal section (Fig. 4B); sectioned material (of whole-mounts, Fig. 4A) confirmed the presence of labeled cells, fibers, and terminals.

Overall, the connections of n.IX-X-Ri were similar in male and female brains. In particular, the connections with DTAM, Rm, nTS, Ri and n.III were not distinguishable (Table 1). Some differences were that the connection with VS was more robust in males than in females, whereas the connection with n.V was more robust in males. In females, labeled cells in ipsilateral Rpd were observed (in addition to terminal fields). The connection from contralateral to ipsilateral n.IX-X was observed in one brain only.

In whole-mounts, a large fiber tract could be seen extending anteriorly from n.IX-X. Fibers that led to DTAM formed a slight genu ventral and caudal to DTAM. Fibers that led to n.III crossed to the contralateral medulla ventral to the cerebellum.

Injections into n.IX-X invariably included a portion of lateral Ri. From this experiment only, it is therefore not possible to determine whether labeled projections originate specifically in n.IX-X or Ri. Projections to and from n.IX-X and DTAM and n.IX-X and rRpd, however, were confirmed with retrograde tracing (see Injections into DTAM and Injections into rRpd sections below).

Injections into DTAM

At the level of the injection (Fig. 5A), labeled cells and terminal fields were present in contralateral DTAM. More ventrally (Fig. 5B), labeled cells were present in ipsilateral n.V. Both labeled cells and fibers were present in Rm and Ri (Fig. 5C), ipsilaterally and

contralaterally. More ventrally (Fig. 5D), labeled cells and terminal fields extended into n.IX-X and cells and fibers were present in n.III, both ipsilaterally and contralaterally, as well as in ipsilateral VS. Most ventrally (Fig. 5E), the ipsilateral dorsal infundibular nucleus (DIN) contained labeled cells and terminal fields. In many brains, sparse and inconsistent labeling was present in thalamic nuclei (data not shown); labeling was usually stronger on the side ipsilateral to the injection. Labeled nuclei included the anterior, central, lateral, posterior, and ventromedial thalamus. In one brain (male), a few (one–three) labeled cells were observed in the APOA on both sides (also not shown).

In general, labeling following injections into DTAM was more robust in males (Table 2). For example, both labeled cells and fibers were present in contralateral DTAM and n.IX-X in males, whereas in females, labeled fibers were observed but labeling in cells was weak or absent. In males, terminal fields were observed in Rpd (on both sides); this pattern of labeling was not present in females. Similarly, projections between DTAM and n.V were robust in males but largely absent in females. In males, the connection with DIN was present contralaterally (although weak); this pattern was not observed in females. In females, a weak connection with VS was present contralaterally but was not observed in males.

In whole-mounts, several fiber tracts could be seen extending ventrally from the injection sites; these spread out both anteriorly and posteriorly to form extensive terminal fields in Rpd. The fiber tract from DTAM to VS was large and discrete, dropping ventrally as it traveled anteriorly and terminating within the nucleus in a large oval group of cells intermixed with terminals (Fig. 1C).

Injections into APOA

The APOA is a midline structure. We, therefore, did not distinguish ipsi-from contralateral connections (Table 3).

Most ventrally (Fig. 6D), both labeled cells and terminal fields were present in the ventral infundibular nucleus (VIN). Immediately dorsal (Fig. 6C), label extended into the DIN, posterior (P)POA, VS, and lateral septum (LS). In more dorsal regions (Fig. 6B), labeled cells and terminal fields were also present in medial septum (MS). A dense terminal field was also present in pallium (P). At this level, discrete labeling confined to the rostral subdivision of the Rpd (rRpd) was present in cells and fibers. Although sparse (Fig. 7), the labeling was present in all brains. The most prominent connection of the APOA was with the anterior thalamus, which contained labeled cells and terminal fields (Fig. 6A).

In whole-mounts, a pronounced fiber tract from APOA to the anterior thalamus could be observed (Fig. 2A), traveling posterolaterally before forming a genu and traveling dorsally into the anterior thalamus. The fibers between APOA and rRpd traveled ventrally and in some cases made a sharp dorsal turn to enter this nucleus (Fig. 7A).

Injections into rRpd

To confirm the projection between rRpd and APOA, we injected rRpd. These injections were made as close to the midline as possible (see Fig. 9A); the approach was lateral. Again, we did not distinguish ipsi- and contralateral distributions of label (Table 4).

Results confirmed a reciprocal connection with APOA (Fig. 8D). Labeled cells and terminal fields were also observed in DIN (Fig. 8D), VS (Fig. 8C), n.IX-X, Ri, and Rm (Fig. 8B,C), as well as in DTAM (Fig. 8A). A terminal field in n.III was present in all brains (Fig. 8C). As was the case for other brain nuclei, label was stronger in male than in female brains, especially retrograde labeling (Table 4); examples include Rpv and Rpd.

A dense terminal field was observed on the ventral surface of the brain, ventral to the injection site in Rpv (Fig. 9A), and descending fibers could clearly be observed traveling dorsal to ventral along the midline in transverse sections (Fig. 9A). Labeled cells and terminal fields were present throughout the thalamus (Fig. 9B); individual fibers could be traced into anterior thalamus (not shown).

DISCUSSION

The sexually differentiated calling patterns of *Xenopus laevis* are conveyed to the vocal organ by a dedicated neuromuscular system that includes laryngeal motor neurons located within cranial nerve nucleus IX-X (Kelley, 2002). The nucleus contains both motor neurons (projecting to muscle) and interneurons (projecting to other CNS neurons). Patch clamp recordings from identified laryngeal motor neurons indicate that although intrinsic membrane and channel properties are sexually differentiated and shape responses to synaptic inputs, these cells do not themselves generate the characteristic rates and patterns of different call types (Yamaguchi et al., 2000). Pattern and rate must instead be driven by the activity of neurons afferent to vocal motor neurons. The goal of this study was to identify these afferent sources and re-examine the issue of whether vocal connectivity in males differs substantially from that in females (as reported in Wetzel et al., 1985).

The use of fluorescent dextran amines and the isolated brain preparation readily permitted identification of anterograde and retrograde connectivity patterns between vocal nuclei, as had been the case for auditory nuclei in *X. laevis* (Edwards and Kelley, 2001). The major findings of this study are the confirmation of a robust and reciprocal connection between n.IX-X and DTAM as well as between DTAM and the ventral striatum, a newly revealed extensive connectivity between the rostral subdivision of the dorsal nucleus raphe and the candidate vocal nuclei described above, and an absence of sexual dimorphism in the connectivity of the candidate vocal nuclei. This last finding is in contrast with previous results using HRP-WGA as a tracer (Wetzel et al., 1985). We did, however, observe that some connections were less robust in female than in male brains.

In addition, several of the retrograde connections previously observed with HRP-WGA were not confirmed, as discussed below. Finally, the pathways connecting candidate vocal nuclei were apparent in the whole-mount preparations. This information should be useful for functional studies of the roles of these brain nuclei in vocal production. It was also helpful in determining whether patterns of labeling were influenced by damage to fibers of passage (as discussed below).

Afferents to n.IX-X

Nucleus n.IX-X is reciprocally connected with DTAM, both contralaterally and ipsilaterally. The contralateral n.IX-X and Ri, as well as Rm on both sides, also project to n.IX-X. Because injection sites into n.IX-X always included a portion of Ri, we could not determine whether ipsilateral Ri is connected to n.IX-X. This information will require intracellular fills of Ri and n.IX-X neurons. More anteriorly, a reciprocal connection with ventral striatum was noted. This connection is probably attributable to adjacent Ri rather than n.IX-X itself as other studies (Marin et al., 1997a,b), also using biotinylated dextran amines in *X. laevis*, noted reciprocal connections between Ri and VS. We noted a projection to Rpd and from n.III as well as reciprocal connections with ipsilateral nTS and contralateral n.V.

Nucleus IX-X contains neurons that project to laryngeal muscle (vocal motor neurons; Kelley, 1980). Do these cells project to DTAM as well? When vocal motor neurons are back-labeled with Lucifer Yellow and DTAM is injected with FR (Zornik and Kelley, 2001), there are no double-labeled somata in n.IX-X. A similar result is obtained after FR

injection into contralateral n.IX-X. Few, if any, triple-labeled cells result when the latter is combined with a third dye injection into DTAM. Nucleus IX-X thus contains three populations of projection neurons: one that exits the CNS to innervate the larynx ipsilaterally, one that projects to DTAM on both sides, and a third that projects to contralateral n.IX-X-Ri (but not directly to motor neurons). For reasons described above, we do not know whether n.IX-X also contains short-axon neurons whose synapses are confined to n.IX-X itself, or adjacent Ri.

In most respects, the pattern of projections to n.IX-X revealed in this study closely resembles previous results (Wetzel et al., 1985), specifically projections from DTAM and contralateral n.IX-X. The projections from n.V and from nTS were also noted previously, although labeled cells in n.III were not observed. Projections to n.IX-X are not distinguishable in the sexes by using either HRP-WGA or FR.

Two caveats to inferring n.IX-X connectivity from this and the previous study are the leakage of injected material into Ri and the possibility that axons severed during tracer application transport FR to terminals or cell bodies. Because n.IX-X is immediately lateral to Ri, avoiding leak-age is not possible. We have instead sought to confirm patterns of connectivity by injections into candidate n.IX-X target brain nuclei. Results of injection into DTAM reveal that this nucleus is indeed reciprocally connected with n.I-X (and also with Ri). What about fibers of passage through n.IX-X? The reciprocal connection between n.IX-X and DTAM is observed with a variety of injection strategies (lateral injections into n.IX-X as per this study; ventral injections into n.IX-X and DTAM as per (Wetzel et al., 1985)). Given that most fiber trajectories are well localized, at least one approach direction should have spared them. Because DTAM is a dorsal nucleus, and because its injections were made with a picospritzer (less likely to damage axons than the minuten pin injections used for n.IX-X injections), labeled cells in n.IX-X are unlikely to be the result of damage to axons traveling through DTAM.

Afferents to DTAM

Nucleus DTAM is the major source of input to the vocal motor nucleus. What are its inputs? One set of afferents arises from a set of interconnected hindbrain nuclei that include projection neurons in n.IX-X and Ri. The second source arises from the forebrain, specifically the ventral striatum. In addition to the reciprocal projection to n.IX-X described above, DTAM also connects to Rpd caudally.

In terrestrial frogs, DTAM has been strongly implicated in the control of vocal behavior. Lesions of DTAM block production of all vocal behaviors (Schmidt, 1966). Electrical stimulation of DTAM at 50 to 100 Hz produces characteristic, well-patterned release calls in terrestrial frogs (Schmidt, 1971). Similarly, nuclei within the lateral tegmental field have been implicated in vocal control in both mammals and birds (Jurgens, 2002). In Schmidt's model of vocal production, DTAM is thought to be responsible for vocal pattern generation in collaboration with neurons of the caudal medulla adjacent to n.IX-X. The rhombencephalic connections described here may subserve a similar function in *Xenopus laevis*. Because the connections between DTAM and rhombencephalic nuclei are reciprocal, activity in Ri, for example, could also contribute to driving DTAM. Additional information on how this set of connections functions during vocal pattern generation could provide useful tests of Schmidt's model.

If activity in DTAM is required for generating vocal behaviors, how, in turn, is it activated? Conspecific calling can provide a powerful stimulus for vocal behaviors in both sexes (Tobias et al., 1998). Auditory responses have been recorded in anuran VS (Mudry and Capranica, 1980), and VS stimulation can alter response properties of neurons in auditory

midbrain (Endepols and Walkowiak, 2001/2). In this study and in others (Marin et al., 1997a,b; DTAM is identified as the parabrachial nucleus), strong reciprocal connections between DTAM and VS are reported. In *X. laevis*, the ventral striatum and nucleus accumbens are also reciprocally connected with auditory thalamic nuclei (Edwards and Kelley, 2001).

DTAM neurons express very high levels of receptor for androgenic hormones (Kelley, 1980; Perez et al., 1996), hormones that are absolutely required for advertisement calling in males (Wetzel and Kelley, 1983). The expression of androgen and estrogen receptors is highly specific for the vocal system in *X. laevis* and, in addition to DTAM, includes laryngeal motor neurons and interneurons, Ri, and VS (Kelley et al., 1975; Morrell et al., 1975). In the auditory midbrain, the laminar nucleus has many steroid-accumulating neurons (Kelley, 1980). This pattern of expression suggests that activation of vocal behaviors by gonadal hormones is effected by means of steroid target nuclei.

In contrast to previous results (Wetzel et al., 1985), we did not observe marked differences in the connections of DTAM in male and female brains. In particular, the projection from n.IX-X to DTAM was observed in both sexes, although less robust in females. Neurophysiological approaches will be required to resolve whether the less consistent results in females reflect sexually differentiated use of DTAM in calling behavior, for example, or whether sparser synaptic connectivity in females is responsible for a reduced uptake of tracers.

We did not observe a direct projection from DTAM to the preoptic area in this study. This projection was reported previously and was confined to males (Wetzel et al., 1985). One possible explanation for the discrepancy in results is transneuronal transport of HRP-WGA (Gerfen et al., 1982). Candidate transfer nuclei include the VS, DIN, and rRpd. The role of the POA in vocal behavior is discussed below.

Anterior preoptic area

The preoptic area plays a central role in the activation of calling in terrestrial frogs. For example, stimulation of this region in intact *Rana pipiens* evokes calling behavior (Schmidt, 1966, 1971, 1973); particularly effective sites were the extreme rostral pole of the POA, the APOA (Wada and Gorbman, 1977). This region contains many cells that express steroid receptors both in *Xenopus* and in *Rana* (Kelley et al., 1975, 1978; Kelley, 1980; di Meglio et al., 1987). Because androgenic stimulation is required for calling, at least in male *Xenopus*, it seemed reasonable to suppose that relatively direct connections between the APOA area and vocal circuitry would be present. Our previous results (Wetzel et al., 1985) were interpreted in light of this expectation. The results of the present study, however, reveal that connections between the APOA and vocal circuitry, if present in the *X. laevis* CNS, are indirect and operate by means of VS or rRpd.

The findings of this study indicate instead that the APOA has substantial connections to telencephalic nuclei (pallium, LS, MS, and VS) and ventral diencephalon (PPOA, DIN, and VIN). The APOA's connection with anterior thalamus was particularly striking. The only caudal projections that we observed (except for spinal cord, which we did not characterize) were to and from rRpd (discussed below). Labeled cells in POA have also been described after injection into pallium in *Discoglossus* (Westhoff and Roth, 2002). A projection from habenula to APOA has been noted in *Rana esculenta* (Kemali et al., 1980).

In addition to a role in evoking vocal behaviors, the anuran APOA is also thought to be a key way station in the process by which acoustic stimulation affects the neuroendocrine system (Wilczynski et al., 1993). Auditory information may access the APOA by means of

VS (whose cells respond to auditory stimuli; Mudry and Capranica, 1980) or by means of the anterior thalamus (which receives projections from the auditory midbrain in *Rana*; Neary and Wilczynski, 1986). The calls of other males (as well as other forms of social contact) can produce elevated androgen levels in tree frogs and cricket frogs (Burmeister and Wilczynski, 2000; Chu and Wilczynski, 2001). Levels of circulating steroids are controlled by gonadotrophin (Gn) secretion which is, in turn, controlled by a network of diencephalic neurons (Allison and Wilczynski, 1991; Wilczynski et al., 1993). Among these are the PPOA, the DIN, and the VIN, which, as we show here, are also connected to the APOA in *X. laevis*. The axons of neurons containing the peptide that controls Gn, Gn releasing hormone, may play neuromodulatory roles elsewhere in the CNS, including vocal centers (Burmeister et al., 2001).

Role of the dorsal raphe

An unexpected result of this study is the extensive connectivity between the small rostral subdivision of the dorsal raphe nucleus (rRpd) and elements of the vocal pathway. The rRpd connects not only with n.IX-X and DTAM but also with various nuclei to which these project such as Ri, Rm, n.V, n.III, DIN, and ventral striatum (the latter result was also reported by Marin et al., 1997a,b).

An inferior/superior subdivision of the raphe was recognized some years ago (van Mier and ten Donkelaar, 1984). A further subdivision of the superior raphe is suggested here by the specificity with which its rostral subdivision (rRpd) projects to elements of the vocal circuitry.

The dorsal nucleus of the raphe is known to provide modulatory influences to locomotor rhythms, and these effects have been elucidated in *X. laevis* tadpoles (Sillar et al., 1992, 1995, 1998). Work in invertebrate ganglia (Beltz et al., 1984; Marder and Bucher, 2001) has established the principle that neuromodulators can reconfigure neural networks for motor behaviors and produce a variety of rhythmic outputs. In addition, as is the case for most and perhaps all vertebrates, the anuran raphe is a major source of serotonergic innervation for the central nervous system. Serotonin is known to affect motoneuron excitability in frogs (Cardona and Rudomin, 1983) and increase excitability of laryngeal motor neurons in mammals (Zealear et al., 2001). The rRpd neurons described here are also likely to be serotinergic and could play an important role in modulating vocal rhythms in *X. laevis*.

In summary, this reinvestigation of vocal circuitry in *Xenopus laevis* highlights a series of candidate nuclei for roles in the generation of vocal behavior. These nuclei are summarized in Figure 10. Plausible hypotheses are that a set of rhombencephalic neurons located in DTAM, Rm, Ri, and n.IX-X are responsible for generating patterned vocal activity, that activity is modulated by neurons in a small nucleus of the dorsal raphe (rRpd), and that activity in VS (particularly that evoked by conspecific calls), together with effects of steroid hormones at many sites in the vocal circuit, contribute to the initiation of calling.

Acknowledgments

Grant sponsor: National Institutes of Health; Grant number: NS23684.

We thank Erik Zornik for useful comments on the article and Andrea Roe for histologic assistance. Ayako Yamaguchi prepared the photomontages of horizontal sections.

Abbreviations

APOA anterior preoptic area

AT	anterior thalamus
DIN	dorsal infundibular nucleus
DTAM	pretrigeminal nucleus of the dorsal tegmental area of the medulla
Hab	habenula
LS	lateral septum
MS	medial septum
NI	nucleus isthmi
n.III	motor nucleus of III (oculomotor)
n.IX-X	motor nucleus of IX-X (glossopharyngeal)
n	motor nucleus of V (trigeminal)
N.V	trigeminal nerve
nTS	nucleus tractus solitarius
P	pallium
POA	preoptic area
PPOA	posterior preoptic area
Ri	reticularis inferior
Rm	reticularis medius
Rpd	raphe pars dorsalis
Rpv	raphe pars ventralis
rRpd	rostral raphe pars dorsalis
VIN	ventral infundibular nucleus
VS	ventral striatum

LITERATURE CITED

Allison JD, Wilczynski W. Thalamic and midbrain auditory projections to the preoptic area and ventral hypothalamus in the green treefrog (*Hyla cinerea*). Brain Behav Evol. 1991; 38:322–331. [PubMed: 1764635]

Beltz B, Eisen JS, Flamm R, Harris-Warrick RM, Hooper SL, Marder E. Serotonergic innervation and modulation of the stomatogastric ganglion of three decapod crustaceans (*Panulirus interruptus*, *Homarus americanus*, and *Cancer irroratus*). J Exp Biol. 1984; 109:35–54. [PubMed: 6376680]

Burmeister S, Wilczynski W. Social signals influence hormones independently of calling behavior in the treefrog (*Hyla cinerea*). Horm Behav. 2000; 38:201–209. [PubMed: 11104638]

Burmeister S, Somes C, Wilczynski W. Behavioral and hormonal effects of exogenous vasotocin and corticosterone in the green treefrog. Gen Comp Endocrinol. 2001; 122:189–197. [PubMed: 11316424]

Cardona A, Rudomin P. Activation of brainstem serotoninergic pathways decreases homosynaptic depression of monosynaptic responses of frog spinal motoneurons. Brain Res. 1983; 280:373–378. [PubMed: 6652498]

Chu J, Wilczynski W. Social influences on androgen levels in the southern leopard frog, *Rana sphenocephala*. Gen Comp Endocrinol. 2001; 121:66–73. [PubMed: 11161771]

di Meglio M, Morrell JI, Pfaff DW. Localization of steroid-concentrating cells in the central nervous system of the frog *Rana esculenta*. Gen Comp Endocrinol. 1987; 67:149–154. [PubMed: 3497838]

Edwards CJ, Kelley DB. Auditory and lateral line inputs to the midbrain of an aquatic anuran: neuroanatomic studies in *Xenopus laevis*. J Comp Neurol. 2001; 438:148–162. [PubMed: 11536185]

Endepols H, Walkowiak W. Integration of ascending and descending inputs in the auditory midbrain of anurans. J Comp Physiol [A]. 2000–2001; 186:1119–1133.

Gerfen CR, O'Leary DD, Cowan WM. A note on the transneuronal transport of wheat germ agglutinin-conjugated horseradish peroxidase in the avian and rodent visual systems. Exp Brain Res. 1982; 48:443–448. [PubMed: 6185358]

Holtzman E, Freeman AR, Kashner LA. Stimulation-dependent alterations in peroxidase uptake at lobster neuromuscular junctions. Science. 1971; 173:733–736. [PubMed: 4327989]

Hosogai M, Matsuo S. Inspiratory neurons with decrementing firing pattern in raphe nuclei of feline medulla. Auton Neurosci. 2002; 99:13–17. [PubMed: 12171251]

Jiang X, Johnson RR, Burkhalter A. Visualization of dendritic morphology of cortical projection neurons by retrograde axonal tracing. J Neurosci Methods. 1993; 50:45–60. [PubMed: 7506340]

Jurgens U. Neural pathways underlying vocal control. Neurosci Biobehav Rev. 2002; 26:235–258. [PubMed: 11856561]

Kelley DB. Auditory and vocal nuclei in the frog brain concentrate sex hormones. Science. 1980; 207:553–555. [PubMed: 7352269]

Kelley, DB. Hormonal regulation of motor output in amphibians; *Xenopus laevis* vocalizations as a model system. In: Pfaff, D.; Etgen, A.; Fahrbach, S.; Rubin, R., editors. Hormones, brain and behavior. San Diego: Academic Press; 2002. p. 445-468.

Kelley, DB.; Tobias, ML. The vocal repertoire of *Xenopus laevis*. In: Hauser, M.; Konishi, M., editors. The design of animal communication. Cambridge: MIT Press; 1999. p. 9-35.

Kelley DB, Morrell JI, Pfaff DW. Autoradiographic localization of hormone-concentrating cells in the brain of an amphibian, *Xenopus laevis*. I. Testosterone. J Comp Neurol. 1975; 164:47–59. [PubMed: 1176651]

Kelley DB, Lieberburg I, McEwen BS, Pfaff DW. Autoradiographic and biochemical studies of steroid hormone-concentrating cells in the brain of *Rana pipiens*. Brain Res. 1978; 140:287–305. [PubMed: 304754]

Kemali M, Guglielmotti V, Gioffre D. Neuroanatomical identification of the frog habenular connections using peroxidase (HRP). Exp Brain Res. 1980; 38:341–347. [PubMed: 6154592]

Luksch H, Walkowiak W, Munoz A, ten Donkelaar HJ. The use of in vitro preparations of the isolated amphibian central nervous system in neuroanatomy and electrophysiology. J Neurosci Methods. 1996; 70:91–102. [PubMed: 8982986]

Marder E, Bucher D. Central pattern generators and the control of rhythmic movements. Curr Biol. 2001; 11:R986–R996. [PubMed: 11728329]

Marin O, Gonzalez A, Smeets WJ. Basal ganglia organization in amphibians: afferent connections to the striatum and the nucleus accumbens. J Comp Neurol. 1997a; 378:16–49. [PubMed: 9120053]

Marin O, Gonzalez A, Smeets WJ. Basal ganglia organization in amphibians: efferent connections of the striatum and the nucleus accumbens. J Comp Neurol. 1997b; 380:23–50. [PubMed: 9073081]

Morrell JI, Kelley DB, Pfaff DW. Autoradiographic localization of hormone-concentrating cells in the brain of an amphibian, *Xenopus laevis*. II. Estradiol. J Comp Neurol. 1975; 164:63–77. [PubMed: 1176652]

Mudry KM, Capranica RR. Evoked auditory activity within the telencephalon of the bullfrog (*Rana catesbeiana*). Brain Res. 1980; 182:303–311. [PubMed: 6965601]

Neary TJ, Northcutt RG. Nuclear organization of the bullfrog diencephalon. J Comp Neurol. 1983; 213:262–278. [PubMed: 6601115]

Neary TJ, Wilczynski W. Auditory pathways to the hypothalamus in ranid frogs. Neurosci Lett. 1986; 71:142–146. [PubMed: 3491346]

Nikundiwe AM, Nieuwenhuys R. The cell masses in the brainstem of the South African clawed frog *Xenopus laevis*: a topographical and topological analysis. J Comp Neurol. 1983; 213:199–219. [PubMed: 6841669]

Perez J, Cohen MA, Kelley DB. Androgen receptor mRNA expression in *Xenopus laevis* CNS: sexual dimorphism and regulation in laryngeal motor nucleus. J Neurobiol. 1996; 30:556–568. [PubMed: 8844518]

Schmidt RS. Central mechanisms of frog calling. Behaviour. 1966; 26:251–285. [PubMed: 5933272]

Schmidt RS. A model of the central mechanisms of male anuran acoustic behavior. Behaviour. 1971; 39:288–317. [PubMed: 5315471]

Schmidt R. Central mechanisms of frog calling. Am Zool. 1973; 13:1169–1177.

Schmued L, Kyriakidis K, Heimer L. In vivo anterograde and retrograde axona transport of the fluorescent rhodamine-dextran-amine, Fluoro-Ruby, within the CNS. Brain Res. 1990; 526:127–134. [PubMed: 1706635]

Sillar KT, Wedderburn JF, Simmers AJ. Modulation of swimming rhythmicity by 5-hydroxytryptamine during post-embryonic development in *Xenopus laevis*. Proc R Soc Lond B Biol Sci. 1992; 250:107–114.

Sillar KT, Woolston AM, Wedderburn JF. Involvement of brainstem serotonergic interneurons in the development of a vertebrate spinal locomotor circuit. Proc R Soc Lond B Biol Sci. 1995; 259:65–70.

Sillar K, Reith CA, McDearmid JR. Development and aminergic neuromodulation of a spinal locomotor network controlling swimming in *Xenopus* larvae. Ann N Y Acad Sci. 1998; 860:318–332. [PubMed: 9928322]

Simpson HB, Vicario DS. Brain pathways for learned and unlearned vocalizations differ in zebra finches. J Neurosci. 1990; 10:1541–1556. [PubMed: 2332796]

Simpson HB, Tobias ML, Kelley DB. Origin and identification of fibers in the cranial nerve IX-X complex of *Xenopus laevis*: Lucifer Yellow backfills in vitro. J Comp Neurol. 1986; 244:430–444. [PubMed: 3958236]

Tobias ML, Kelley DB. Vocalizations by a sexually dimorphic isolated larynx: peripheral constraints on behavioral expression. J Neurosci. 1987; 7:3191–3197. [PubMed: 3668623]

Tobias ML, Marin ML, Kelley DB. Development of functional sex differences in the larynx of *Xenopus laevis*. Dev Biol. 1991; 147:251–259. [PubMed: 1879611]

Tobias ML, Viswanathan SS, Kelley DB. Rapping, a female receptive call, initiates male-female duets in the South African clawed frog. Proc Natl Acad Sci U S A. 1998; 95:1870–1875. [PubMed: 9465109]

van Mier P, ten Donkelaar HJ. Early development of descending pathways from the brain stem to the spinal cord in *Xenopus laevis*. Anat Embryol (Berl). 1984; 170:295–306. [PubMed: 6335361]

Wada M, Gorbman A. Mate calling induced by electrical stimulation in freely moving leopard frogs, *Rana pipiens*. Horm Behav. 1977; 9:141–149. [PubMed: 303606]

Westhoff G, Roth G. Morphology and projection pattern of medial and dorsal pallial neurons in the frog *Discoglossus pictus* and the salamander *Plethodon jordani*. J Comp Neurol. 2002; 445:97–121. [PubMed: 11891656]

Wetzel DM, Kelley DB. Androgen and gonadotropin effects on male mate calls in South African clawed frogs, *Xenopus laevis*. Horm Behav. 1983; 17:388–404. [PubMed: 6662518]

Wetzel DM, Haerter UL, Kelley DB. A proposed neural pathway for vocalization in South African clawed frogs, *Xenopus laevis*. J Comp Physiol [A]. 1985; 157:749–761.

Wilczynski W, Allison JD, Marler CA. Sensory pathways linking social and environmental cues to endocrine control regions of amphibian forebrains. Brain Behav Evol. 1993; 42:252–264. [PubMed: 8252377]

Yamaguchi A, Kelley DB. Generating sexually differentiated vocal patterns: laryngeal nerve and EMG recordings from vocalizing male and female African clawed frogs (*Xenopus laevis*). J Neurosci. 2000; 20:1559–1567. [PubMed: 10662845]

Yamaguchi A, Kaczmarek LK, Kelley DB. Intrinsic membrane properties of laryngeal motoneurons that control sexually differentiated vocal behavior in African clawed frogs, *Xenopus laevis*. Biol Bull. 2000; 199:175–176. [PubMed: 11081721]

Zealear DL, Swelstad MR, Sant'Anna GD, Bannister RA, Billante CR, Rodriguez RJ, Garren KC, Billante MJ, Champney MS. Determination of the optimal conditions for laryngeal pacing with the

Itrel II implantable stimulator. Otolaryngol Head Neck Surg. 2001; 125:183–192. [PubMed: 11555752]

Zornik E, Kelley DB. Identifying interneurons in the vocal motor nucleus of *Xenopus laevis*. Soc Neurosci Abstr. 2001; 88:18.

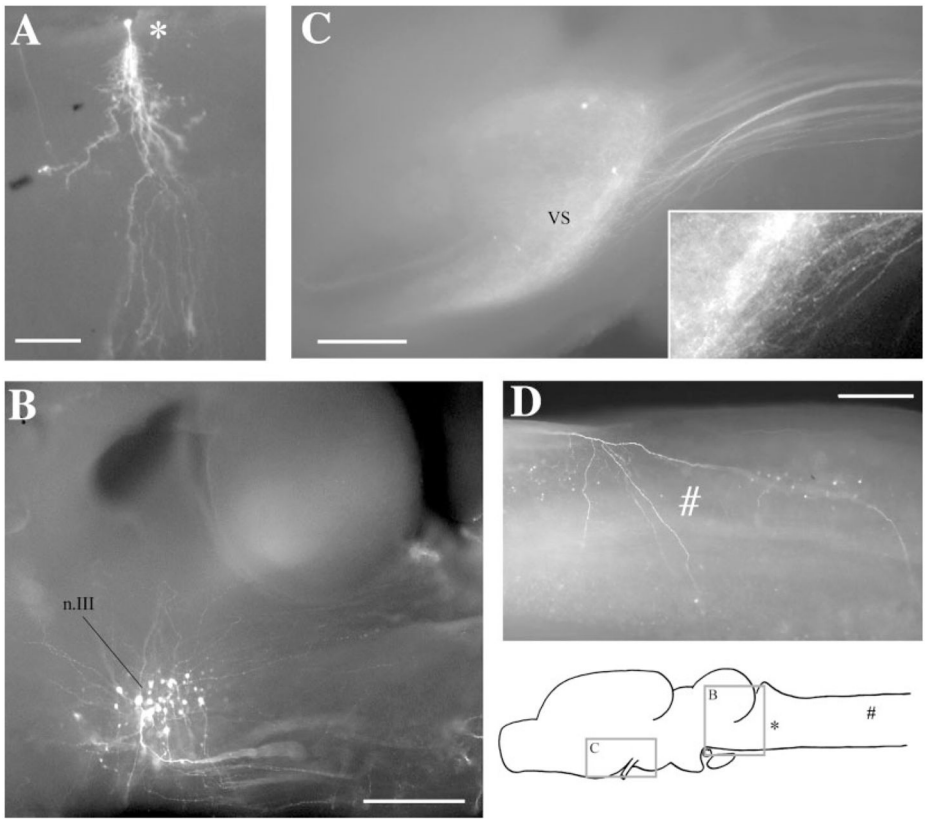

Fig. 1.

Whole-mount preparations. **A:** A labeled cell in the Rpd after a discrete injection into rRpd. **B:** Labeled cell bodies in n.III after an injection into n.IX-X. Dendrites can be seen extending dorsoanteriorly and dorsoposteriorly. Posteriorly, labeled axons can be seen fasciculating ventrally before crossing to the contralateral side of the brain. **C:** Labeled terminal fields and cells in VS after an injection into DTAM. The projecting fiber tract can be seen posteriorly. Synaptic boutons and terminating fibers can be seen in the enlargement (insert). **D:** A labeled terminating fiber (#) in the medulla after an injection into DTAM. The locations of areas shown in C and B, the labeled cell in A, and the fiber in D are indicated on the sagittal diagram. For abbreviations, see list. Scale bars = 300 μm in A–D.

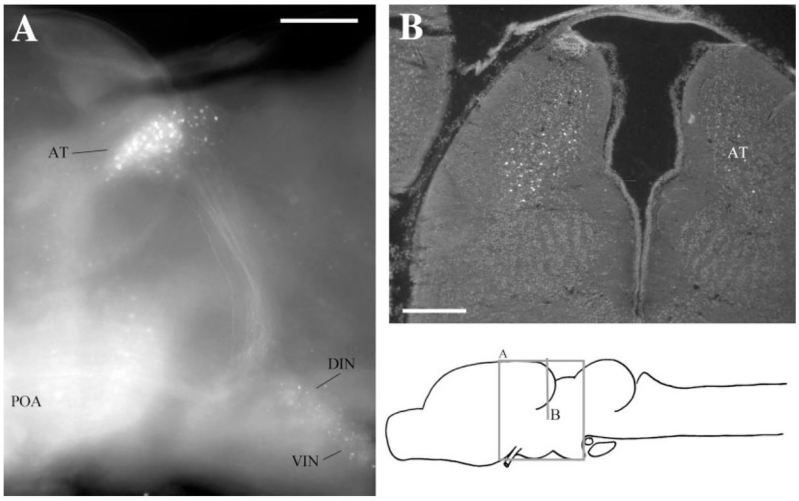

Fig. 2.

Label in AT after injecting APOA. **A:** Sagittal view in whole-mount showing labeled cells in AT, DIN, VIN, and POA as well as the projecting fiber tract to AT. **B:** Transverse section through AT. For abbreviations, see list. Scale bars = 300 μm in A,B.

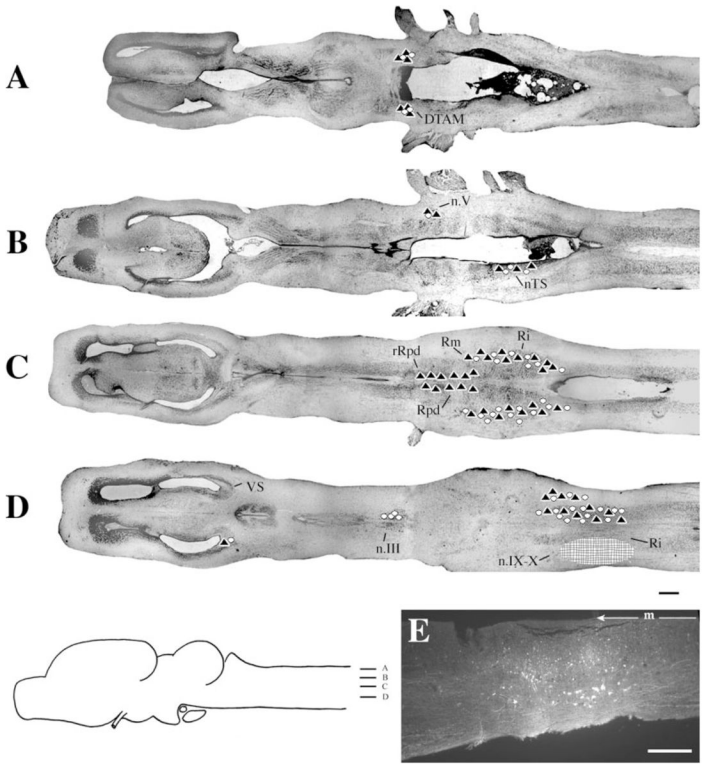

Fig. 3.

Injections into n.IX-X. **A–D:** Black triangles indicate labeled terminal fields; white circles indicate labeled cells; the hatched area indicates the location and extent of a typical injection site. **E:** Photomicrograph of a typical injection site. m, midline. For other abbreviations, see list. Scale bar = 500 μm in D (applies to A–D), 300 μm in E.

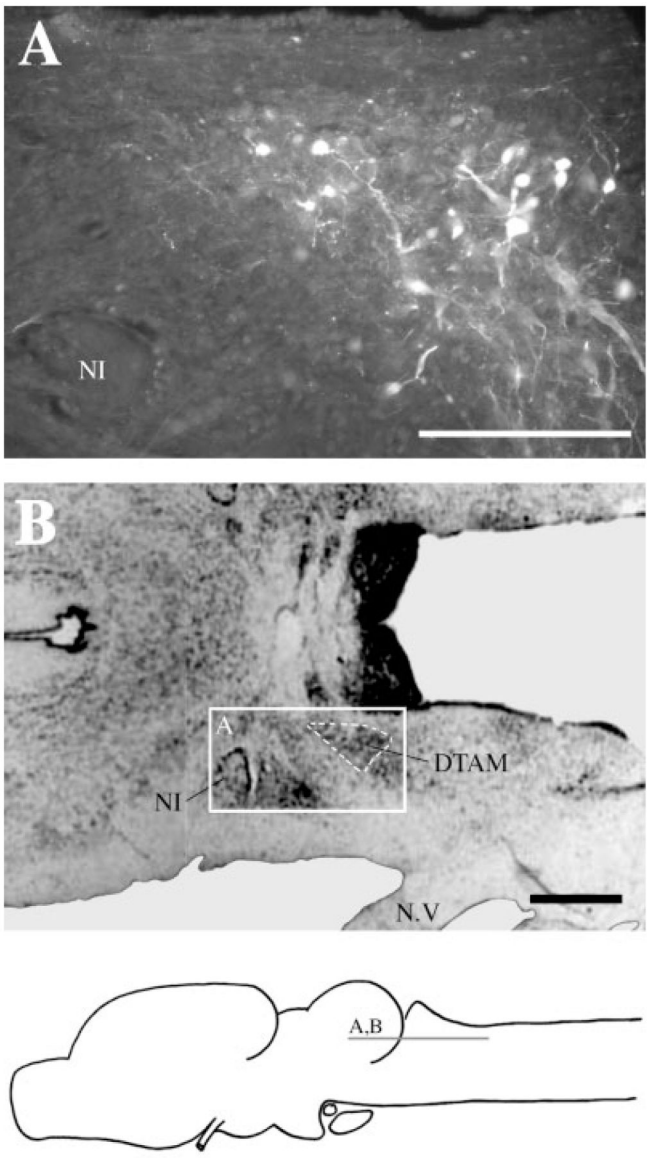

Fig. 4.

Label in DTAM after Fluoro-Ruby injections into n.IX-X. **A:** Labeled cells, fibers, and synaptic boutons in a horizontal section. **B:** Reference cresyl-violet–stained horizontal section through DTAM. For abbreviation, see list. Scale bar = 300 μm in A, 500 μm in B.

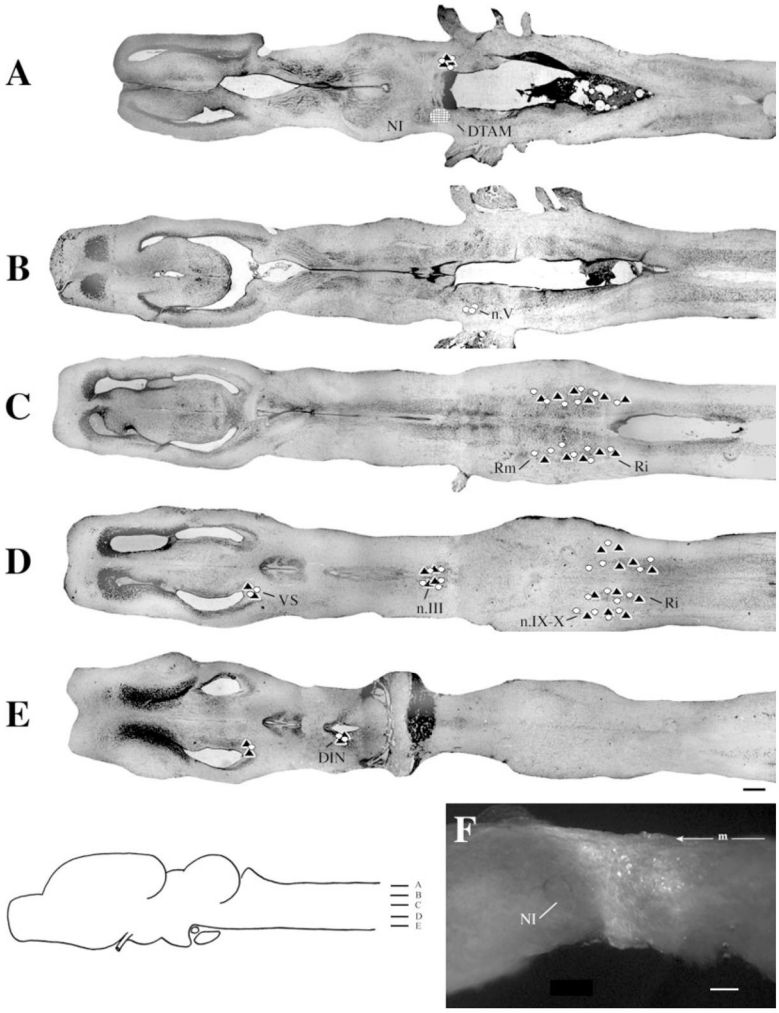

Fig. 5.

Injections into DTAM. **A–E:** Symbols and scale bar as in Figure 3. **F:** Photomicrograph of a typical injection site. m, midline. For other abbreviations, see list. Scale bar = 300 μm in F.

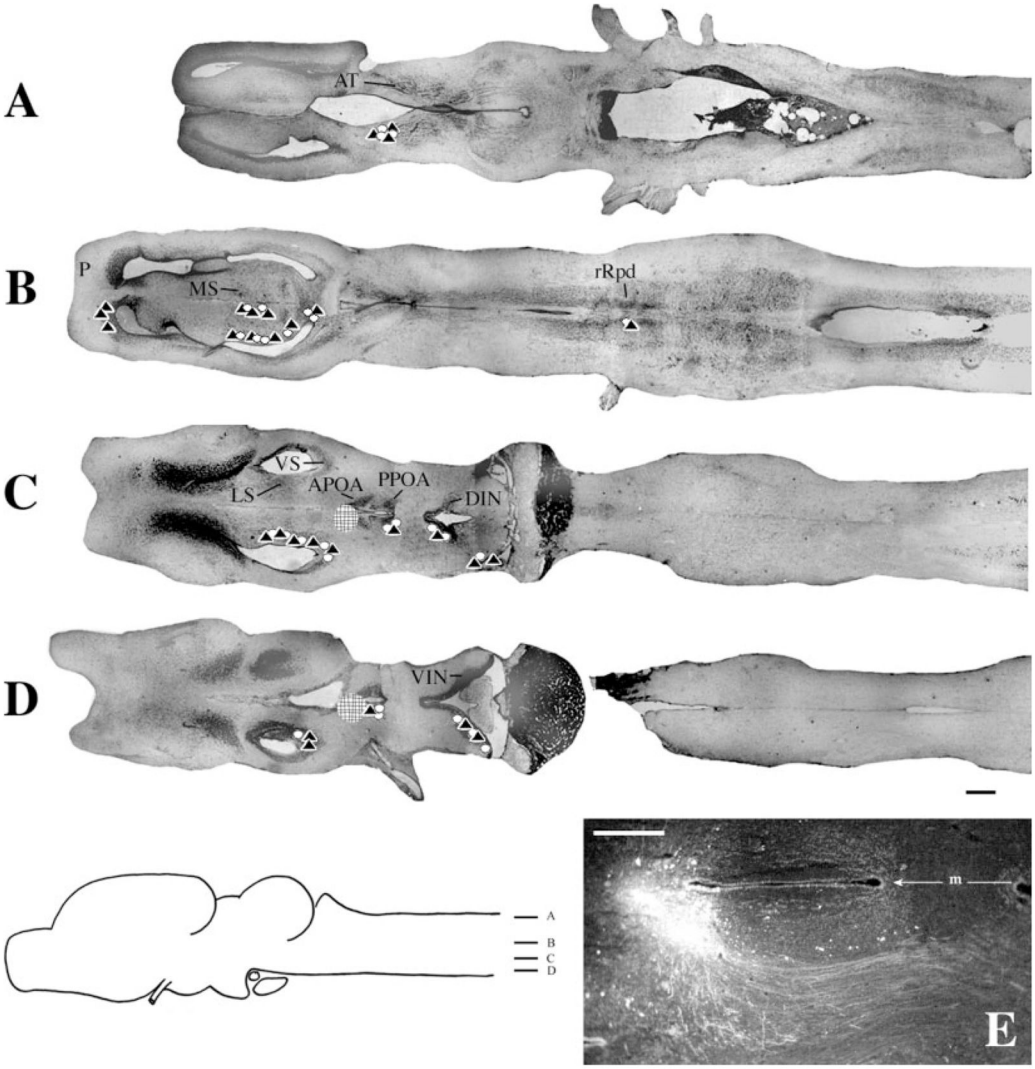

Fig. 6.

Injections into APOA. **A–D:** Symbols and scale bar as in Figure 3. **E:** Photomicrograph of a typical injection site. m, midline. For other abbreviations, see list. Scale bar in E = 300 μm in E.

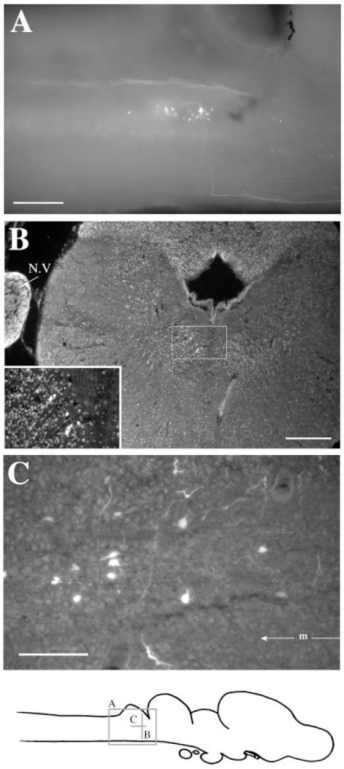

Fig. 7.

Label in rRpd after Fluoro-Ruby injections into APOA. **A:** Sagittal view in whole-mount. A labeled fiber can be seen traveling along the ventral surface from APOA and making a right-angled turn beneath the cerebellum and rRpd. **B:** Transverse section with labeled cells in rRpd. The insert is an enlargement of the boxed area and clearly shows seven labeled cells in rRpd. **C:** Labeled cells and fibers in a horizontal section through rRpd. m, midline. For other abbreviations, see list. Scale bars = 300 μm in A,B, 100 μm in C.

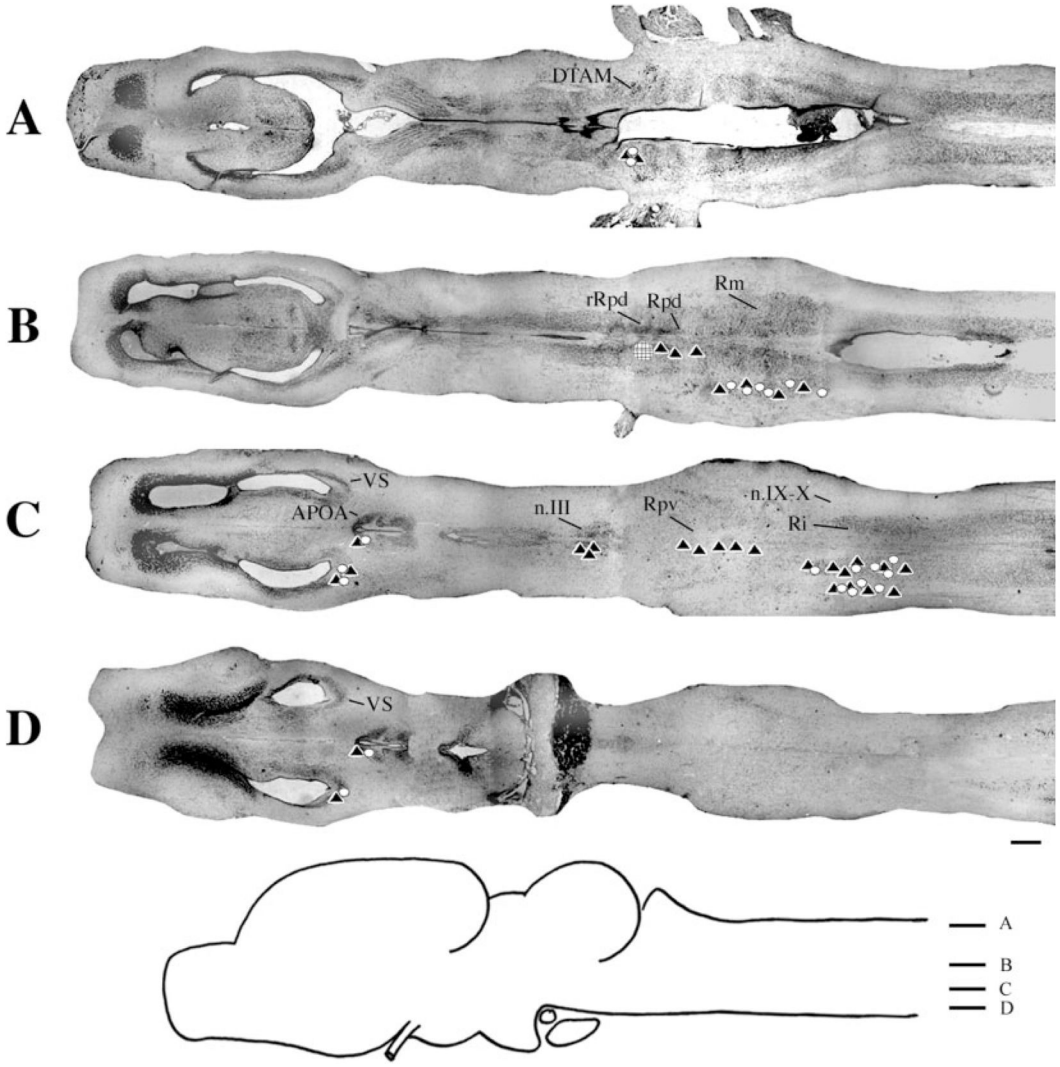

Fig. 8.

Injections into rRpd. Symbols and scale bar as in Figure 3. A typical injection site is illustrated in Figure 9A. For abbreviations, see list.

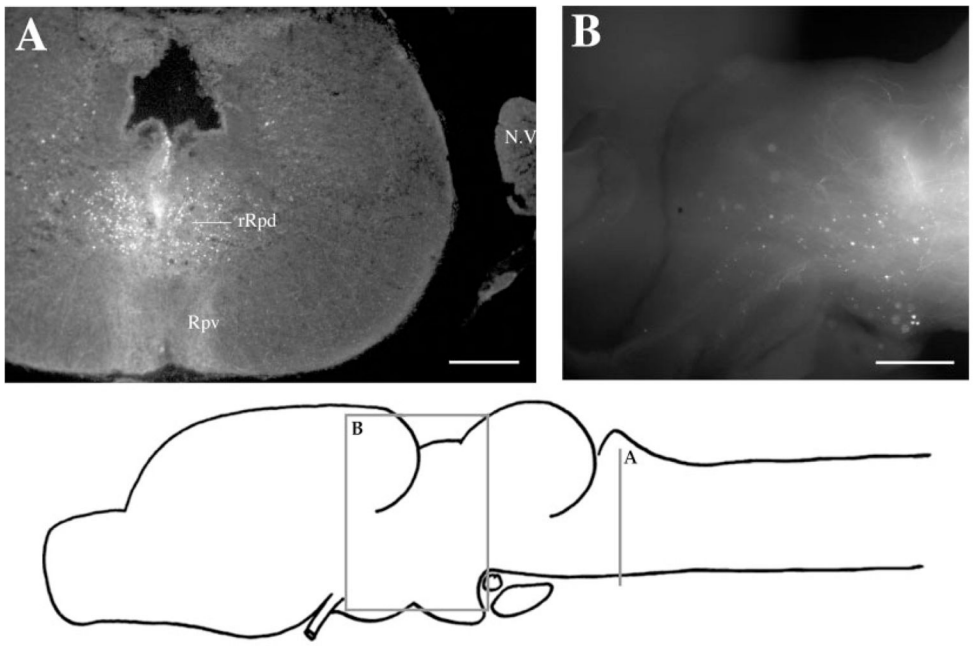

Fig. 9.

Label after Fluoro-Ruby injections into rRpd. **A:** Transverse section through the injection site, showing dense terminal fields in Rpv. **B:** Labeled cells and terminal fields in the thalamus in whole-mount. For abbreviations, see list. Scale bars = 300 μm in A,B.

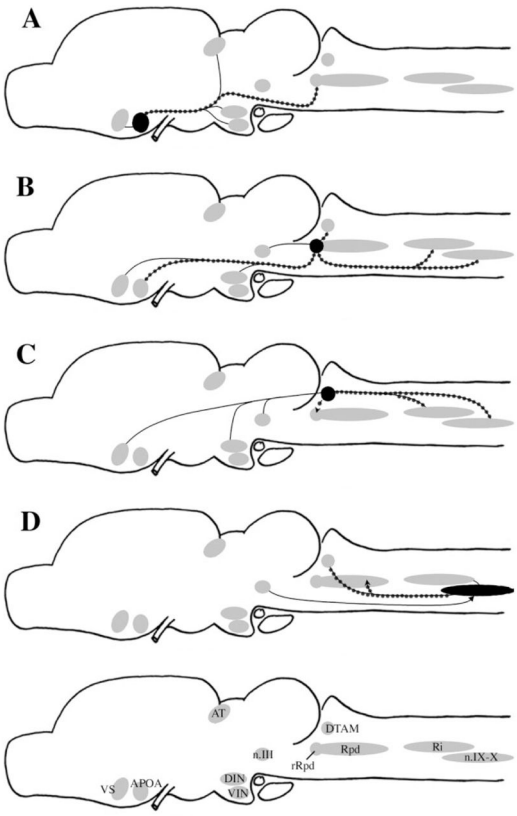

Fig. 10.

Summary diagrams of results of injections into APOA (**A**), rRpd (**B**), DTAM (**C**), and n.IX-X (**D**). Plain lines indicate reciprocal connections. Dotted lines indicate projections that were confirmed by retrograde labeling. Arrows indicate direction of nonreciprocal projections. For abbreviations, see list.

TABLE 1

Injections into n.IX-X[1]

		M (Total injections: 4)		F (Total injections: 5)			M (Total injections: 4)		F (Total injections: 5)	
		Cells	TF	Cells	TF		Cells	TF	Cells	TF
VS	Ipsilateral	●●	●●	○○○○	●	Contralateral	—	—	—	—
n.III		—	—	—	—		●●●●	—	●●●●●	—
n.V		—	—	—	—		●○	●●	●●●●○	●●●●●
DTAM		●●●●	●●●●	●●●●●	●●●●●		●●●●	●●●●	●●●●●	●●●●●
Rpd		—	●●●	●●●	●●●●●		○	●●●	○	●●●●●
Rpv		●●○○	—	●●●●○	—		●○	—	—	—
Rm		●●●●	●●●●	●●●●●	●●●●●		●●●	●●●	●●●●●	●●●●●
Ri		●●●●	●●●●	●●●●●	●●●●●		●●●●	●●●●	●●●●●	●●●●●
n.IX-X		IS	IS	IS	IS		●●●●	●●●●	●	●●●●●
nTS		●●●●	●●●●	●●●●●	●●●●●		—	—	—	—

[1]In this and all subsequent tables, each dot represents one injected brain. A black dot indicates labeling throughout the nucleus. A white dot indicates one to three filled cells or terminating fibers. Dashes indicate an absence of labeling. Ipsilateral and contralateral are respective to the injection site. M, male; F, female; IS, injection site; TF, terminal fields. For all other abbreviations, see list.

TABLE 2

Injections into DTAM[1]

		M (Total injections: 3)		F (Total injections: 3)			M (Total injections: 3)		F (Total injections: 3)	
		Cells	TF	Cells	TF		Cells	TF	Cells	TF
VS		●○	●●●	●●●	●●●		—	—	●○	●
DIN		●○	○	●●○	●		●○	●○	—	—
n.III		●●	●●●	●	●●		●●	●●●	●	●●
DTAM		IS	IS	IS	IS		●●	●●○	○○	●●●
n.V	Ipsilateral	●●●	●●●	●	—	Contralateral	—	—	—	—
rRpd		—	●●●	—	—		—	●●○	—	—
Rm		●●	●●○	●○○	●○○		●●	●●○	○○	●○○
Ri		●●●	●●	●○○	●●●		●●●	●●	●●	●●●
n.IX-X		●●	●●●	●○○	●●●		●●○	●●●	●	●●●

[1]See footnote to Table 1.

TABLE 3

Injections into APOA[1]

	M (Total injections: 5)		F (Total injections: 5)	
	Cells	TF	Cells	TF
Pallium	—	●●●●	—	●●●●
LS	●●●●●	●●●●●	●●●●●	●●●●●
MS	●●●●●	●●●●●	●●●●	●●●●
VS	●●●●●	●●●●●	●●●●●	●●●●●
PPOA	●●●●●	●●●●●	●●●●	●●●●
DIN	●●●●●	●●●●●	●●●●	●●●●
VIN	●●●●●	●●●●●	●●●●●	●●●●●
Hab	—	●●●●	—	●●●●●
AThal	●●●●●	●●●●●	●●●●●	●●●●
rRpd	●●●○	●●○	●●●○○	●○○

[1] See footnote to Table 1.

TABLE 4

Injections into rRpd[1]

	M (Total injections: 4)		F (Total injections: 3)	
	Cells	TF	Cells	TF
VS	●●●●	●●	●○	●●
APOA	●○○○	●●	○○	●●●
DIN	●●●	●●●	●●	●●●
n.III	○	●●●●	●●●	●●●
DTAM	●	●	●○○	●●●
n.V	●●●	●●●	●●○	●●○
Rpd	●	●●●●	—	●
Rpv	●	●●●●	—	●
Rm	●●●●	●●●●	●●●	●●●
Ri	●●●○	●●●●	●○	●●●
n.IX-X	●●○○	●●●●	●	●○○

[1]See footnote to Table 1.